72nd International Astronautical Congress (IAC), Dubai, United Arab Emirates, 25-29 October 2021.

IAC-21-B1.5.3

SOCIAL BENEFITS ASSESSMENT OF EARTH OBSERVATION MISSIONS THROUGH THE SDG2030

C. Zuliani*[a], V. Santoro[b], M. Nugnes[c], C. Colombo[d]

[a] *Department of Aerospace Science and Technology, Politecnico di Milano, Via La Masa 34, Milan, Italy, 20156*, chiara.zuliani@mail.polimi.it
[b] *Department of Aerospace Science and Technology, Politecnico di Milano, Via La Masa 34, Milan, Italy, 20156*, valerio.santoro@mail.polimi.it
c *Department of Aerospace Science and Technology, Politecnico di Milano, Via La Masa 34, Milan, Italy, 20156*, marco.nugnes@polimi.it
d *Department of Aerospace Science and Technology, Politecnico di Milano, Via La Masa 34, Milan, Italy, 20156*, camilla.colombo@polimi.it
* Corresponding Author

Abstract

The 2030 Agenda for Sustainable Development, subscribed by all the United Nations Member States in 2015, provides a shared direction towards a sustainable thriving of the humankind and the planet. The Agenda lists 17 goals, the Sustainable Development Goals (SDGs), which state a path to be followed by all the countries within 2030 for a global development. Earth orbiting satellites and especially Low Earth Orbit
(LEO) satellites lie in a privileged location to monitor our planet. This allows Earth observation (EO) missions to contribute to the achievement of the SDGs, as extensively recognised by both space agencies and the UN.

In this paper, a new methodology is presented to provide agencies, governments and stakeholders a tool to assess the societal benefits of EO missions. The proposed approach aims at quantifying the social value rating of the missions through the achievement of the SDGs. For this purpose, nine services provided to Earth by EO missions have been identified: Built-up land (i.e. all kinds of man-made constructions), Agriculture, Wild nature, Geology, Limnology, Oceanography, Meteorology, Air Quality Monitoring and Hazards Monitoring. Following the work of Scalera et al, the evaluation of the social benefits is carried out by introducing four indices relating satellite payloads to these services, which are linked to the SDGs. The four indices focus on the payloads and orbit main characterising factors: temporal resolution, spatial resolution, spectral efficiency and Earth coverage.
The dissertation is currently limited to repeating Sun-synchronous circular low Earth orbits, which represent the majority of EO missions, and both passive and SAR-sensors are analysed. The investigation can also be rearranged as a tool to maximise the social outcome of a mission during its design phase.

The model is applied to the Copernicus program and a few more missions, to assess their contribution to the achievement of the SDG2030. In general, passive instruments show a higher versatility in terms of social performances, while SARs gain better scores but focused on fewer goals.
Keywords: GNSS, SDG 2030, satellite constellations, sustainability

1. Introduction

In the last years, the aerospace sector is experiencing a thriving period. The advent of its privatisation and commercialisation, the enabling of breakthrough technologies, the constant raising awareness of the benefits and opportunities that space technologies can provide to the societies have led to coin the expression space economy. Space economy refers to the entire value chain that, starting from research, development, and manufacturing of enabling space infrastructures (the so-called upstream) goes up to the production of innovative enabled services (downstream). For what concerns economic benefits, there were many institutions and organisations, such as the European Space Agency (ESA) or the Organisation for Economic Co-operation and Development (OECD) among the others, whose aim has been to assess both the direct and indirect returns that space activities provide to governments and communities.

Societal impact assessments coming from space activities have been overlooked over years, and the reasons are the intrinsic difficulty in assessing something not directly measurable, such as human wellbeing, and a societal structure focused more on an economic growth perspective rather than on a societal thriving. In the last years, a common need of promoting social welfare policies is arising and the new-born concept of the

Wellbeing Economy is proof. A wellbeing economy starts from the idea that public interests should determine economics and not the other way around, monitoring and valuing health, nature, education and communities. In this context, the Sustainable Development Goals (SDGs) can provide the necessary guidelines to lead countries through this transition. It is well known nowadays that space activities play a key role in providing added value services to governments and communities. As described in the following sections, this study aims at developing a tool for quantitatively evaluating the social outcomes of Earth observation (EO) missions through the SDGs.

The subject of the social and economic value of space missions has been largely examined in the past few years. Indeed, many space programs and agencies currently work on the definition of a framework to assess the contribution of EO missions to the SDGs or to define the socio-economic value of space missions. To cite a few, the initiative EO4SDG of the Group on Earth Observation (GEO) works closely with the UN on the social outcomes of Earth observation missions, the Committee on Earth Observation Satellites (CEOS) works with governments, scientists, academia for the development of partnerships for the implementation of the SDGs, the United Nations Committee of Experts on Global Geospatial Information Management (UN-GGIM) follows the same target working closely with the statistical community. ESA has commissioned a comprehensive analysis of the concrete contribution that can be given to the SDGs by EO missions. The United Nations Office for Outer Space Affairs (UNOOSA) has examined the contribution that EO and Global Navigation Satellite System (GNSS) missions can give to the SDGs identifying key activities for each Goal in a qualitative way.

The current work revises the work made by Scalera and contributes to obtaining more accurate indices and results. The latter identifies eight EO services and their monitoring requirements are compared with missions' performance according to temporal resolution, spatial resolution, spectral efficiency and Earth coverage. Then, a method to assess the social value of remote sensing missions is defined. Although the chosen indices of the current dissertation coincide with the ones developed in the previous paper, these have been developed differently.

The paper is organised in the following manner. In Sec. 2 the modelling of the different figures of merit used for the indices computation is introduces, while in Sec. 3 the proposed model is applied to Copernicus program for validation. Finally, Sec. 4 concludes the paper.

2. Modelling

In this chapter, the indices modelling, and validation are presented. The indices are set starting from the identification of several mission features capable of answering fundamental questions on the monitoring service, such as:

- When is the monitoring of the service performed?
- Where is the monitoring of the service performed?
- What services are monitored by the payload?
- How well are the services observed by the sensor?

According to these questions, respectively the temporal resolution, Earth coverage, spectral efficiency and spatial resolution indices are figured out and discussed in the following sections.

2.1 Spatial resolution index

Spatial resolution is a measure of the smallest object that can be resolved by the sensor, or the ground area imaged through the of the sensor, or the linear dimension on the ground represented by each pixel. The Instantaneous Field Of View (IFOV) is the angle corresponding to the actual area the instrument or antenna can see at a given moment. The figure of merit chosen to model the spatial resolution index of passive sensors is the *Ground Sample Distance* (GSD), corresponding to the elementary size of the ground surface measured by the instrument. To be distinguished, a ground element must have a dimension greater than - or equal to - the pixel size so that differences from one detector to the next reveal the presence of that element.

The spatial resolution of a Synthetic Aperture Radar (SAR) system is more complex. The resolution across-track is primarily controlled by the effective pulse duration, whereas the resolution along-track is generated using an engineering approach explained in this section.

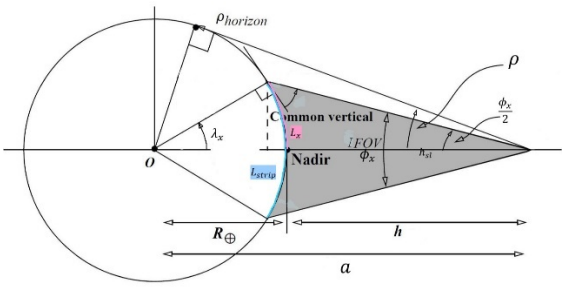

Fig. 1. Pushbroom geometry. Graphically adapted from Vallado

2.1.1 Pushbroom sensors

Pushbroom sensors use a line imager which covers the full swath width. Each element of the detector corresponds to a pixel on-ground. The inputs needed to compute the GSD of a pushbroom sensor are listed in Table. The semi-major axis is the only orbital parameter, while the other inputs are sensor specifications.

Table 1. Inputs for pushbroom sensor spatial resolution

Input variable	Description	Unit of measurement
a	Semi-major axis	[km]
D_t	Payload System aperture	[m]
N_{pix}	Number of pixels of detector element	[-]
λ_{max}	Maximum operative wavelenght	[m]
Φ_x	Element IFOV aperture in cross-track direction	[deg]

The reference geometry for the calculations is shown in Fig. 1. In the figure, in addition to the already introduced geometric variables, the total length on the ground of the strip, L_{strip}, is depicted.

The altitude, h, and Earth angular radius, ρ, are computed as:

$$h = a - R_{\oplus} \tag{1}$$

$$\rho = \sin^{-1}\frac{R_{\oplus}}{h + R_{\oplus}} \tag{2}$$

Then, the central angle, λ_x, corresponding to half of the IFOV is evaluated according to Eq. (3). For the pushbroom sensor the IFOV corresponds to the whole line of pixels.

$$\tan\left(\frac{\Phi_x}{2}\right) = \frac{\sin(\rho)\sin(\lambda_x)}{1 - \sin(\rho)\cos(\lambda_x)} \tag{3}$$

At this point the corresponding linear distance on the ground, L_x, and the total length on the ground of the strip, L_{strip}, are computed as:

$$L_x = R_{\oplus}\lambda_x \tag{4}$$

$$L_{strip} = 2L_x \tag{5}$$

Finally, the resolution limited by the pixel size is obtained and converted into meters.

$$\mathrm{Res}_{pix} = \frac{L_{strip}10^3}{N_{pix}} \tag{6}$$

The resolution limited by diffraction is given by Eq. (7), where in the pushbroom case h_{sl} is always equal to the altitude.

$$\mathrm{Res}_{diff} = \frac{2.44 h_{sl} 10^3 \lambda_{\max}}{D_t} \tag{7}$$

Finally, the GSD is selected conservatively as the maximum value between the resolutions obtained in Eqs. (6) and (7).

2.1.2 SAR sensors

With regard to SAR sensors, the spatial resolution is modelled only for the Stripmap mode. The spatial resolution of the sensors operating in ScanSAR mode is not modelled, because it does not depend only on the sensor specifications. Instead, it is taken as input for the index development. The Spotlight mode is not considered, because it is only used in certain situations and the location of the observed region is not known in advance, making the Earth coverage index evaluation impossible.

The resolution is computed both in the along-track direction, called *azimuth resolution*, and in the cross-track direction, the so-called *range resolution*. In the azimuth resolution, the antenna dimension plays the main role. In the range direction, high resolution can be achieved by considering adequate pulse shape and signal processing. The inputs needed for the computation of SAR spatial resolution are listed in Table 2.

Table 2. Inputs for SAR sensor spatial resolution model

Input variable	Description	Unit of measurement
L_{az}	Antenna azimuthal length	[km]
η	Look angle	[m]
B	Bandwidth	[deg]

The range resolution, δ_r, according to Karbhari and Ansari [26], is computed as:

$$\delta_r = \frac{c}{2B\sin(\eta)} \tag{8}$$

where c corresponds to the speed of light (c= 2.997·108 m/s), B stands for the pulse bandwidth and η is the look angle, described as the angle between the SSP and the slant range. The geometry shown in Fig. 2 represents the observed region of a SAR in Spotlight mode, highlighting the azimuth and range resolutions.

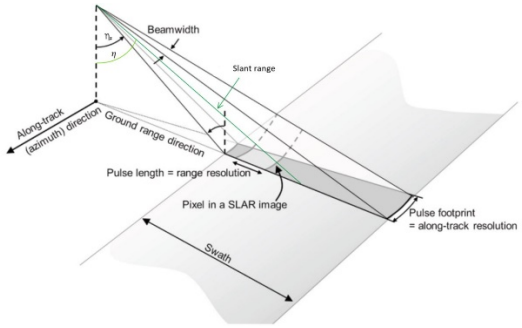

Fig. 2. SAR geometry. Graphically adapted from NASA SAR handbook

The azimuth resolution is simply equal to half of the antenna length, L_{az}.

$$\delta_a = \frac{L_{az}}{2} \tag{9}$$

It should be noted that the azimuth resolution is independent of the altitude and a short antenna yields a fine along-track resolution. To be conservative, the maximum value between the range and azimuth resolution is considered for the index evaluation.

2.1.3 Index development

Each service defined has different requirements in terms of Spatial Resolution (SR). In other words, the object of the observation requires different values of GSD to be detected and to furnish the appropriate information to the sensor.

The minimum and maximum SR requirements for each service are listed in Table 3. All the requirements can be found in the mentioned literature. Average values have been selected when several requirements for a service were present. For what concerns the *Air Quality Monitoring* (AQM) service, the range has been extracted both from Veefkind and from the examination of several sensors focused on AQM.

Table 3. Spatial resolution requirements for each EO service

Service	$SR_{service,min}$	$SR_{service,max}$
Built-up land	0.1	100
Agriculture	1	100
Wild Nature	3	100
Geology	10	1500
Limnology	2	500
Oceanography	40	25000
Meteorology	90	9000
Air Quality Monitoring	250	10000
Hazards Monitoring	7	1000

The space resolution index I_{SR} is obtained comparing the spatial resolution of the services and the computed one of the payload. The index is computed as:

$$I_{SR} = \frac{SR_{service,\max} - SR_{payload}}{SR_{service,\max} - SR_{service,\min}} \tag{10}$$

where $SR_{service,max}$ and $SR_{service,min}$ respectively represent the maximum and the minimum spatial resolution requirements for the concerned service and, on the other side, $SR_{payload}$ stands for the payload computed resolution. In the case of a SAR operating in ScanSAR mode, the payload resolution $SR_{payload}$ is not computed but is instead an input to the index calculation. The services requirements are shown in Fig. 3. On the y-axis, the services are listed. On the x-axis, their corresponding required GSD intervals are reported.

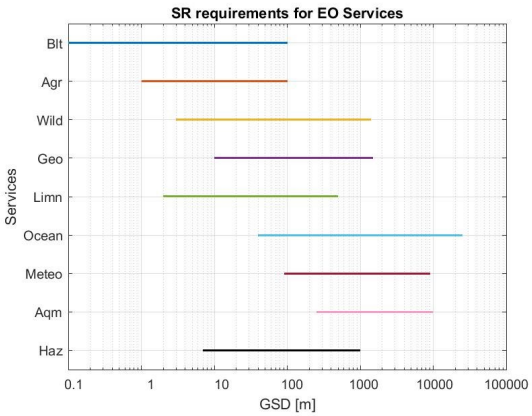

Fig. 3. Spatial Resolution Requirements for each EO service

2.2 Temporal resolution index

As previously mentioned, satellite missions devoted to the observation of the Earth commonly use repeated ground track orbits. This class of orbits is identified with the so-called ReVisit Time (RVT), that is the time elapsed between two successive observations of the same ground point on the surface of the Earth.

This situation mathematically occurs after a repeat cycle period, but it may occur in a shorter period if allowed by the swath width and tilt angle of the sensor. Indeed, a strong correlation exists between the sensor properties and the RVT.

2.2.1 Passive sensors swath

The pushbroom and whiskbroom swath widths were modelled in the same way, according to the hypothesis that the whiskbroom swath width is scanned in the time interval the Sub-Satellite Point (SSP) moves down one ground pixel length.

Having defined the altitude, h, and the angular radius, ρ, according to Eq. (2) and, the angle, η, detecting the farthest point on the ground with respect to the SSP, and the elevation angle, ε, can be determined as:

$$\eta = \frac{FOV}{2} + \vartheta_{tilt} \tag{11}$$

$$\varepsilon = \cos^{-1}\left(\frac{\sin\eta}{\sin\rho}\right) \tag{12}$$

where ϑ_{tilt} represents the tilt angle of the spacecraft. At this point, the Earth central angle, λ, is computed according to Eqs. (13) or (14), respectively, whether $\varepsilon > \varepsilon_{min}$ or $\varepsilon < \varepsilon_{min}$, where ε_{min} can be set as the minimum elevation angle acceptable for the mission purposes. It rarely happens that $\varepsilon < \varepsilon_{min}$, but if it is the case, the ε_{min} is set to 20° according to typical minimum elevation angle values for EO purposes.

$$\lambda = \frac{\pi}{2} - \eta - \varepsilon \tag{13}$$

$$\lambda = \frac{\pi}{2} - \eta - \varepsilon_{\min} \tag{14}$$

Finally, the swath width, S_{width}, is derived.

$$S_{width} = 2\lambda R_{\oplus} \tag{15}$$

To get a more accurate result, the apparent inclination, i', is introduced according to Luo. The apparent inclination is the angle between the equator and the ground track of the satellite in the Earth-Centred Earth-Fixed (ECEF) system, and for circular orbits i' is defined as:

$$\tan(i') = \frac{\sin i}{\cos i - \frac{1}{Q}} \tag{16}$$

where Q is a parameter denoting the number of revolutions completed per day. The inclination, i, is computed according to Curtis in Eq. (17), taking into account the second zonal harmonic J_2 and having set a Sun-synchronous nodal precession rate, $\dot{\Omega}$, equal to the mean motion of the Earth about the Sun.

$$i = \cos^{-1}\left(-\frac{2\,\dot{\Omega}\, a^{\frac{7}{2}}}{3\sqrt{\mu}\, J_2\, R_{\oplus}} \right) \tag{17}$$

The swath of the satellite on the equator S'_{width} can then be calculated as follows:

$$S'_{width} = \frac{S_{width}}{\sin i'} \tag{18}$$

In Table 4 a resume of the needed inputs for the passive sensor swath width modelling is presented.

Table 4. Inputs for passive sensors swath width model

Input variable	Description	Unit of measurement
a	Semi-major axis	[km]
ϑ_{tilt}	Tilt angle	[deg]
FOV	Field of view	[deg]
$\dot{\Omega}$	Nodal precession rate	[deg/s]

2.2.2 SAR sensors swath

Concerning the SAR swath width, it is worth reminding that these sensors only observe off-nadir ground regions. For this reason, the internal and external look angles, η_I and η_E, are introduced.

Knowing the satellite altitude, the ground distances, d_I and d_E, related to η_I and η_E can be easily computed as follows:

$$d_{I,E} = R_{\oplus}\lambda_{I,E} \tag{19}$$

where the internal and external Earth central angles, $\lambda_{I,E}$ are computed as:

$$\lambda_{I,E} = \frac{\pi}{2} + \eta_{I,E} + \varepsilon_{I,E} \tag{20}$$

In Eq. (21), the internal and external elevation angles, $\varepsilon_{I,E}$, are computed as:

$$\varepsilon_{I,E} = \cos^{-1}\left(\frac{\sin\eta_{I,E}}{\sin\rho} \right) \tag{21}$$

where the angular radius, ρ, is:

$$\rho = \sin^{-1}\left(\frac{R_{\oplus}}{h + R_{\oplus}} \right) \tag{22}$$

At this point, the swath width results as:

$$S_{width} = d_E - d_I \tag{23}$$

and the same procedure of Eq. (18) is followed to get S'_{width}.

In Table a resume of the needed inputs for SAR sensors swath width modelling is presented, and in Fig. 4 a representation of the mentioned variables can be appreciated.

Table 5. Inputs for SAR sensors swath width modelling

Input variable	Description	Unit of measurement
a	Semi-major axis	[km]
η_I	Internal look angle	[deg]
η_E	External look angle	[deg]

The modelling of the RVT has been addressed according to a novel technique proposed by Luo et al., assuming repeating Sun-synchronous orbits and J_2 orbital perturbation. The model derivation is not here reported, following this the cited technique.

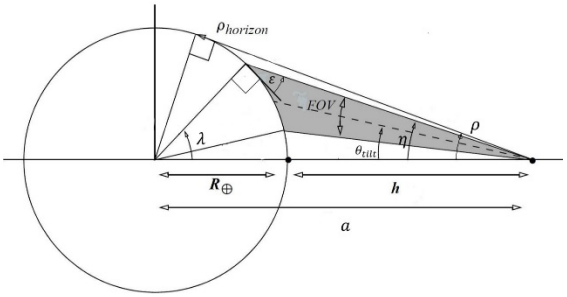

Fig. 4. Passive sensors geometry for swath width computation. Graphically adapted from Vallado.

2.2.3 Index development

The temporal resolution index is obtained following the same conceptual procedure as for the space resolution index. In this case, the RVT is the parameter the index is based on. According to the literature, indicative ranges of RVT values required by the services considered are listed in Table 6. Agriculture values have been set according to Lancheros. Limnology boundaries have been set according to Sentinel-3 mission requirements, while for AQM the range has been assessed according to the revisit time of several missions devoted to the tropospheric air quality monitoring. The other requirements have been averaged among the literature values. The requirements are shown in Fig. 5, where on the y-axis are the services and on the x-axis the required RVT intervals.

Table 6. Revisit time values required for each EO service

Service	$RVT_{service,min}$	$RVT_{service,max}$
Built-up land	1 year	10 years
Agriculture	1 day	8 days
Wild Nature	1 day	365 days
Geology	1 year	10 years
Limnology	1 day	30 days
Oceanography	1 day	180 days
Meteorology	≤ 1 day	5 days
Air Quality Monitoring	≤ 1 day	4 days
Hazards Monitoring	≤ 1 day	7 days

As it can be appreciated, the required $RVT_{service}$ values range from less than one day up to years. For the development of the temporal resolution index, I_{TR}, it is assumed that the lower the operative revisit time $RVT_{operative}$ the better is. The index formulation is presented in Eq. (24), where $RVT_{operative}$ is the modelled mission RVT.

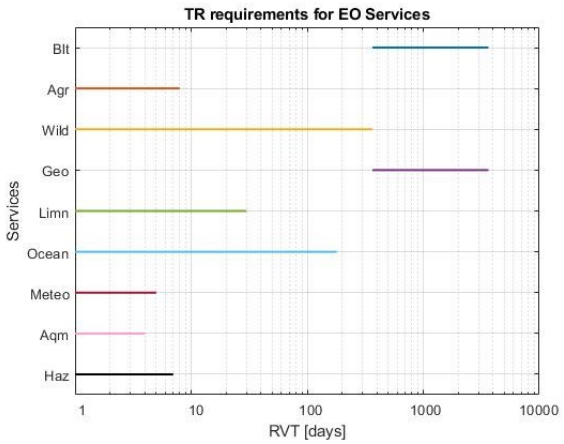

Fig. 5. Temporal resolution requirements for each EO service

$$I_{TR} = \frac{RVT_{service,\max} - RVT_{operative}}{RVT_{service,\max} - RVT_{service,\min}} 100 \qquad (24)$$

Again, if $RVT_{operative}$ exceeds the maximum or minimum $RVT_{service}$, the I_{TR} value is set respectively to 0 or 100, leading always to $0 \leq I_{TR} \leq 100$.

For the computation of the temporal resolution index, inputs come both from orbital parameters and sensor specifications. For the latter, the type of sensor that is analysed (passive or SAR) leads to different inputs, as can be appreciated in the figure. The sensor specifications lead to the computation of the swath width, that, together with the orbital parameters, allows the computation of the RVT. Comparing the RVT to the services temporal resolution requirements, the index is obtained through Eq. (24).

2.3 Spectral efficiency index

The spectral efficiency modelling and index development are carried out in this section both for passive and active sensors.

2.3.1 Passive sensors

The Sun provides a source of energy exploited by passive payloads used for Earth observation. Depending on the wavelength of the electromagnetic spectrum, the Sun's energy is either reflected, as it happens for visible wavelengths, or absorbed and then re-emitted in the form of heat, as it is for thermal infrared wavelengths.

According to the differences among the wavelengths, the spectral efficiency index modelling for passive sensors, $I_{spectre}$, is carried out differently for the VISible and ShortWave InfraRed (VIS-SWIR) and for the Thermal InfraRed (TIR), which are the main operative bands of passive sensors. The Ultra Violet (UV) spectral band is used mostly for detecting gases and belongs to the AQM service. Each passive sensor shall be evaluated

both in the VIS-SWIR and in the TIR domains, hence the two indices obtained shall be merged into one.

The VIS-SWIR ranges from 0.37 μm to 2.5 μm [13]. In this band, the main parameter to define the interaction between the sensor and the Earth surface is reflectivity, representing the percentage of reflected energy for the total incident radiation. The modelling of the index required the definition of spectral signatures in the VIS-SWIR for every EO service basing on the major constituents of such services.

For the Wild nature service, calcite, kaolinite and quartz do not enter the arithmetic mean as the other entries. Indeed, these three elements represent rocks, hence, only their average enters the final service mean. Another clarification concerns the

Hazards monitoring service that includes monitoring of earthquakes, cyclones, floods, droughts, fires and volcanos. Earthquakes monitoring is vital where people are at risk. Since the Built-up land service includes all man-made constructions, which implies the presence of people, the final graph of the Built-up land service (formed by asphalt, concrete, brick etc.) has been selected as the earthquakes element of the Hazards monitoring spectral signature.

Droughts are represented by the dry mud and the golden dry grass, which are averaged and then inserted into the hazards arithmetic mean. The same has been done for quartz, pyroxene basalt and dust, all the three considered for volcanos. Marsh water (40%) enters the mean as representative of the floods; melting snow enters the mean for what concerns cyclones and finally, post-fire burnt forests enter as representative of fires. It is worth recalling that the services constituents have been selected by the authors, according to literature and experience.

The United States Geological Survey (USGS) Spectral Library provides the plot and the dataset of the reflectance values of each material in the VIS-SWIR band. An example of the plot provided by the library can be appreciated in Fig. 6. On the x-axis, the wavelengths ranging from 0.37-2.5 μm are reported, while the vertical axis denotes the reflectance coefficient.

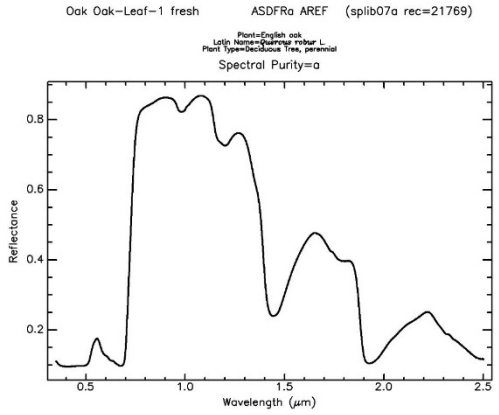

Fig. 6. Spectral signature of a fresh oak leaf

The annexed data is a text file containing all the values of the reflectance coefficient. For most of the materials, 2051 values are corresponding to a linear subdivision of wavelengths from 0.37 μm to 2.5 μm. However, some of them (the constituents of agriculture and oceanography) are text files with 244 entries and their associated 244 values of wavelengths. In some cases, certain entries of the vector of reflectance coefficients are "Not a Number" (NaN). These events have been filled using linear interpolation because in such a way the final plot of the material exactly coincides with the plot furnished by the USGS Spectral Library. The results of the services final reflectance plots are shown in Fig. 7.

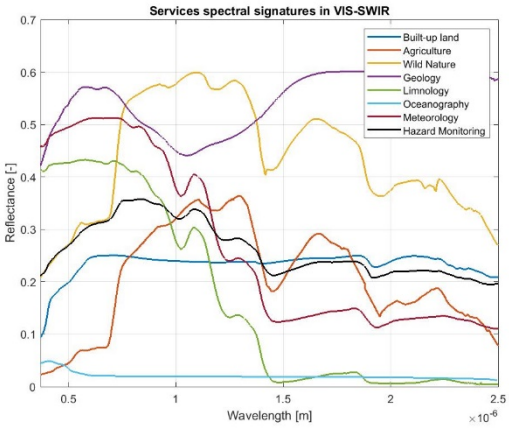

Fig. 7. EO services spectral signatures in VIS-SWIR band

The AQM index is based on the absorption wavelengths of the main pollutants, and therefore the first step is to define them. The largest part of air pollution sources come from human activities, such as fuel combustion from motor vehicles, heat and power generation, industrial facilities, municipal and agricultural waste sites and waste incineration or burning or residential cooking, heating, and lighting with polluting fuels. The main pollutants, according to the World Health Organisation (WHO) and Korotcenkov,

are carbon monoxide (CO), carbon dioxide (CO_2), particulate matter (PM), nitrogen dioxide (NO_2), sulphur dioxide (SO_2), formaldehyde (HCHO), ozone (O_3), methane (CH_4), hydrogen sulphide (H_2S) and ammonia (NH_3).

There are preferable wavelengths for gas detection, mostly in the UV band but also in both the VIS-SWIR and TIR. The gases detectable in the UV and VIS-SWIR wavelength band and the relative wavelengths where they can be detected are reported in Table 7. The main references for the definition of the wavelengths are the *Handbook of Gas Sensor Materials* and the World Meteorological Organisation (WMO).

Table 7. Gases detectable in the UV and VIS-SWIR wavelength band relative wavelengths

Pollutant	Wavelenght for detection [μm]
Carbon monoxide	1.55, 2.33
Carbon dioxide	1.57, 2.01
Particulate matter	0.469, 0.55, 0.67, 1.24
Nitrogen dioxide	0.22, 0.4, 0.496
Methane	1.3, 1.65, 2.3
Hydrogen sulphide	1.57
Ozone	0.254,0.34,0.6
Sulphur dioxide	0.35
Formaldehyde	0.35
Ammonia	2.25

There is no strict definition of the TIR domain. Kuenzer states that the domain extends from 3 μm to 14 μm. However, the mapping of the Earth surface is only possible in the 3-5 μm range, as well as in the 8-14 μm range due to atmospheric windows, where there is relatively high transmittance of terrestrial thermal radiation by atmospheric gases. The second interval has a limited absorption band from 9 to 10 μm caused by ozone, which is omitted by most TIR satellite sensors. Signals recorded in the 3-5 μm window during the day could be contaminated by reflected sunlight.

The emitted radiation is recorded in the TIR domain, while in VIS-SWIR domain reflected radiation is recorded. The parameter chosen to describe the relationship between the sensor and the Earth surface is the *emissivity*. The process followed to develop the index is analogue to the one observed for the VIS-SWIR band, although based on the emissivity instead of the reflectance. Hence, the first step of the process is again to define the spectral signatures of the services in the TIR band, as described in the following section.

The emissivity data in the TIR domain are obtained from the ECOsystem Spaceborne Thermal Radiometer Experiment on Space Station (ECOSTRESS) Spectral Library. As previously done for the VIS-SWIR band, a list of materials has been selected for each service. The materials selected from the USGS library do not coincide with the materials of the ECOSTRESS library, however, the choice has been made as close as possible. As for the VIS-SWIR domain, the AQM does not enter the list because the index is developed differently from the other ones.

As for the previous domain, some entries are averaged and then inserted into the arithmetic mean of the service. This is the case of:

- Calcite, kaolinite and quartz (Wild nature - rocks).
- Soil mollisol and tap water (Hazards monitoring - floods).

The Built-up land final layer enters the arithmetic mean of the Hazards monitoring service for the monitoring of earthquakes. The ECOSTRESS library furnishes both the plots and the dataset of the reflectance values of each material in the TIR wavelengths. When radiation is incident onto a solid object, it can be reflected, absorbed, or transmitted according to the relation:

$$1 = \alpha + \rho + \tau \tag{25}$$

where α, ρ, and τ are the absorption, reflection, and transmission coefficients. On the other hand, the Kirchhoff law states that the absorption coefficient α, under several assumptions considered valid for our materials, is equal to the emissivity coefficient ε. The transmission coefficient of most materials included in the analysis is considered equal to zero, however, for the tap water and the seawater it is equal to 0.543 and for the avena and the bromus it is equal to 0.18.

A built-in Matlab function returns, for each material, the reflectance values, and the corresponding wavelengths. Finally, the emissivity values of the services are obtained subtracting from the total (100%) the reflectance and the transmission in percentage. The results of the services spectral signatures are shown in Fig. 8 and Fig. 9.

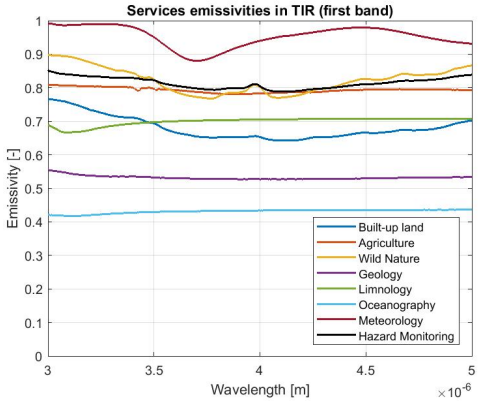

Fig. 8. EO services spectral signature in TIR band 3-5 μm

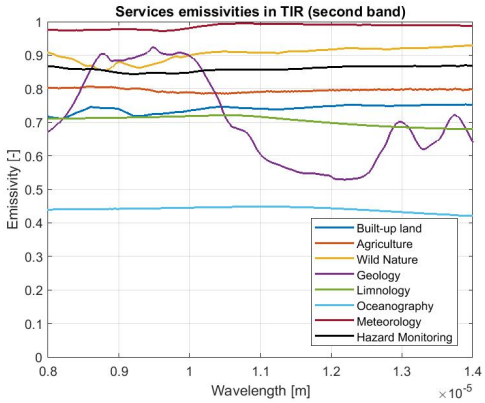

Fig. 9. EO services spectral signature in TIR band - 14 µm

The AQM service has been dealt with as the VIS-SWIR domain. For what concerns this region, the detectable gases and the relative wavelengths where they can be detected are reported in Table 8.

Table 8. Gases detectable in the TIR wavelength band and relative wavelengths

Pollutant	Wavelength for detection [µm]
Carbon monoxide	4.6, 4.8
Carbon dioxide	4.26, 13
Methane	3.2 – 3.5
Hydrogen sulphide	3.72, 3.83
Formaldehyde	3.6
Ammonia	3.03

2.3.2 SAR sensors

The appearance of a SAR image is influenced both by sensor parameters and environmental factors, such as surface roughness. In the derivation of the spectral index for these sensors, two aspects are considered: signal polarisation and wavelengths. These are accounted for as features of the instruments, while each service is classified in terms of surface scattering to deem environmental factors.

The radar signals penetrate deeper as the sensor wavelength increases. Radar sensors deal with longer wavelengths than optical sensors analysed above, at the centimetre to meter scale. Hence, the ability to see through clouds. Because of this property, the Meteorology and Air Quality Monitoring services are not included in the SAR analysis. From a careful literature the commonly used bands in SAR systems and their applications related to the EO services have been derived. When analysing SAR instruments, the wavelength is a fundamental feature to consider because it determines the interaction between the signal and the surface, and the penetration depth into a medium. For example, an X-band radar, operating at a wavelength of about 2.5 - 4 cm, has very little capability to penetrate the broadleaf forest, and thus mostly interacts with leaves at the top of the tree canopy. An L-band signal, on the other hand, with a wavelength of 15 - 30 cm, achieves greater penetration into a forest and allows for more interaction between the signal and large branches and tree trunks.

SARs are active instruments, and they are endowed with their source of illumination. This allows controlling and exploiting the polarisation of the signal on both the transmit and the receive paths. *Polarisation* describes the orientation of the plane of oscillation of a propagating signal. In *linearly polarised* systems, the orientation of the plane of oscillation is constant along the propagation path of the wave, which happens for most of today's sensors. They transmit horizontally and/or vertically polarised wave forms. Single-polarised sensors support only one linear polarisation: they mainly operate in HH-polarisation (horizontal polarisation on transmit; horizontal polarisation on receive) or VV-polarisation (vertical transmit; vertical receive). However, single-polarised sensors may transmit one linear polarisation and receive the other (e.g., HV: horizontal transmit; vertical receive). Over the years, dual-polarisation or quad-polarisation capabilities arose. The last one provides HH-, HV-, VH-, and VV-polarised imagery simultaneously. It is to note that the hypothesis of monostatic configuration is assumed in this analysis, hence the scattering amplitudes of the cross-polarisations are equal. In SAR remote sensing the majority of the polarimetric systems is operated in a monostatic mode.

The different polarisations interact differently with the ground. For what concerns SAR data, there are indeed three main types of scattering, presented in Fig. 10:

- rough surface scattering, which is most sensitive to VV-polarisation.
- volume scattering, which is most sensitive to cross-polarisation (VH or HV).
- double bounce scattering, most sensitive to HH polarised signals.

The scattering strength by polarisation is reported in Table 9.

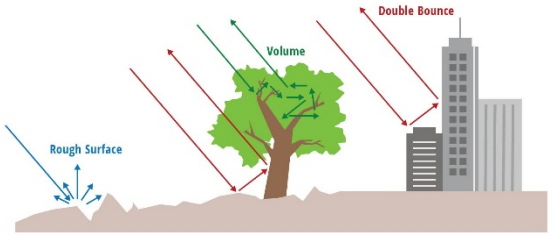

Fig. 10. Main scattering types

Table 9. Relative scattering strengths by polarisation

Relative scattering strength by polarisation	
Rough surface scattering	VV>HH>HV or VH
Double bounce scattering	HH>VV>HV or VH
Volume scattering	HV or VH >HH or VV

2.3.3 Index development

In this section, the index development is carried out for all the services, separating the process to compute the AQM spectral index that differs from the other services. For all the services the input for the computation of the spectral efficiency index I_{spectr} is the operative band - or operative bands - of the sensor in the VIS-SWIR region. The index aims at quantifying the efficiency of the operative wavelengths concerning the services spectral signatures plot.

Supposing a fictitious sensor operating in the wavelengths from 0.5 μm to 0.85 μm and from 1.7 μm to 2.2 μm, the computation of the index is based on the comparison between the areas shown in Fig. 11, which reports the Wild nature spectral signature.

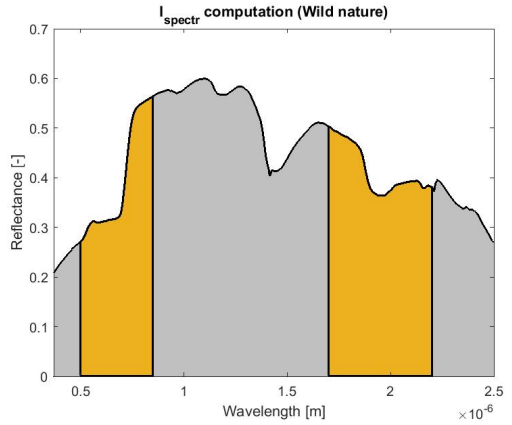

Fig. 11. I_{spectr} computation for Wild nature service for fictitious sensor

The index is based on the ratio between the area under the reflectance plot inside the operative wavelength region, named $A_{operative}$, which is the yellow area in Fig. 11, and the total area underneath the reflectance plot of the service, named $A_{service}$, which is the sum of the yellow and the grey areas of the plot. To be consistent with the formulation of the other indices, the ratio among the two areas is then turned into a percentage. Therefore, the index can be defined as:

$$I_{spectr} = \frac{A_{operative}}{A_{service}} 100 \tag{26}$$

For the AQM service, the operative wavelengths of the sensor are still the input, however, the index is computed differently. Every air is preferably detectable at specified wavelengths. In case one or more *detection wavelengths* of a certain gas lay within one of the intervals of the operative wavelengths of a sensor, the gas is considered as *seen* by the sensor. The model considers the number of gases, n_{gases}, seen by the sensor out of the ten total detectable gases in the UV and VIS-SWIR ranges (CO, CO_2, PM, NO_2, CH_4, HCHO, O_3, O_2, H_2S, NH_3) as:

$$I_{spectr,AQM} = \frac{n_{gases}}{10} 100 \tag{27}$$

In this case, the index is based on a boolean variable, and it is not proportional to the observed area.

For all the services except AQM, the reflectance values of several materials characterising the eight services are retrieved. Through the weighted average of these values, the services spectral signatures are computed and plotted. The input for the index development is the sensor operative wavelength, which allows an area-proportional assessment that leads to the computation of the spectral efficiency index. For the AQM service, the input is the sensor operative wavelength, which is compared to the absorption wavelengths of the main pollutants detected in the VIS-SWIR domain. Basing on a boolean variable, the spectral efficiency index is computed.

The index development for TIR region follows the same path as the VIS-SWIR domain and it is computed differently for the AQM service. The input is still the operative band of the sensor in the treated domain. The index is computed as the previous one, however in this case the areas lay under the emissivity plots of the services and not the reflectance ones. The definition of the index, as for the VIS-SWIR domain, remains:

$$I_{spectr} = \frac{A_{operative}}{A_{service}} 100 \tag{28}$$

Because the TIR domain is split into two parts, the function returns an index for the first interval and another one for the second interval. Then, the two indices are averaged to obtain only one index for each service in the TIR domain. It is possible to give different importance to the two indices setting different values to the two weights, whose sum must always be equal to the unity. Default values are both 0.5 leading to an unweighted average.

Concerning the AQM service, the index is computed as it was in the VIS-SWIR region. Indeed, the index is based on the number of gases, n_{gases}, that can be detected by the sensor out of the six total detectable gases in the TIR range (CO, CO_2, H_2CO, CH_4, H_2S, NH_3). Therefore, the index is computed as:

$$I_{spectr,AQM} = \frac{n_{gases}}{6} 100 \tag{29}$$

For all the services except AQM, the emissivity values of several materials characterising the services are retrieved. Through the weighted average of these values,

the services spectral signatures are computed and plotted. The input for the index development is the sensor operative wavelength, that allows an area-proportional assessment leading to the computation of the spectral efficiency index. For the AQM service, the input is the sensor operative wavelength, which is compared to the absorption wavelengths of the main pollutants detected in the TIR domain. Basing on a boolean variable, the spectral efficiency index is computed.

It can happen that one or more sensors on-board the satellite operates both in the VIS-SWIR and in the TIR domains. In this case, the indices are computed separately for the two intervals, leading to an index $I_{spectr,VISSWIR}$ for the visible and short-wave infrared band, and an index $I_{spectr,TIR}$ for the thermal infrared band for each service. Then, the two indices are merged with a weighted average. The weights are obtained proportionally to the intervals of the sensor of each domain, so that, as an example, a sensor operating for 90% in the TIR domain, has a weight of 0.1 for the VIS-SWIR index and a weight of 0.9 for the TIR band index.

For SAR sensors, wavelength and polarisation of the sensor are the inputs to the spectral index I_{spectr}. To better understand the correlation between the two and the development of the index, first, the link between the services and the polarisation is described exploiting the types of scattering reported in Table 9.

A score from 0 to 2 has been assigned by the authors to each service for every type of scattering basing on the main features of the service (e.g., for the Built-up land service a score of 2 has been assigned to the double bounce because of the manufacture of the buildings). The scores are given according to experience, basing on considerations coming from Fig. 10. The interval of scores has been selected to grant a differentiation between the types of scattering in a service. The results are reported in Table 10.

Table 10. Scores assigned to each service for every type of scattering

Service	Rough surface	Double bounce	Volume
Built-up land	1	2	0
Agriculture	2	0	1
Wild nature	2	1	2
Geology	2	1	0
Limnology	2	2	0
Oceanography	2	0	0
Hazards	2	2	2

A score has been given to each polarisation basing on the "preferred" type of scattering, turning the inequalities of Table into numbers. The scores have values ranging from 1 to 3 and are reported in Table 11.

At this point, it is necessary to correlate the input represented by the polarisation and the services. Each single-polarisation is linked to each service by multiplying its scores of Table 11 and the relative ones of Table 10, adding them up and then normalising to the maximum obtainable score of such service. For example, the score related to the HH polarisation for the Built-up land service is 0.89, which is obtained by multiplying 2

Table 11. Scores assigned to each polarisation for every scattering

Polarisation	Rough surface	Double bounce	Volume
HH	1	2	0
HV	2	0	1
VH	2	1	2
VV	2	1	0

(HH score for Rough surface) by 1 (Built-up land score for Rough surface), then multiplying 3 (HH - Double bounce) by 2 (Built-up land - Double bounce), and multiplying 1 (HH - Volume) by 0 (Built-up land - Volume). The three numbers are summed and divided by 9, which is the sum of the scores of the considered service of Table multiplied by the maximum polarisation score, which is 3. Hence:

$$0.89 = \frac{2 \cdot 1 + 3 \cdot 2 + 1 \cdot 0}{9} \tag{30}$$

In the same way the score of the cross-polarisation (HV or VH) for the same service would be:

$$0.33 = \frac{1 \cdot 1 + 1 \cdot 2 + 3 \cdot 0}{(1+2) \cdot 3} \tag{31}$$

As previously mentioned, the polarisation can be dual or quad. In this case, the results of the two (or four) single-polarisations simultaneously provided are added up. For example, in the previous Built-up land example, in the case of a dual-polarisation HH-HV, the score would be 1.22, given by $0.89 + 0.33$.

These scores need to be turned into percentages to be consistent with the other indices. This operation is performed assuming that the quad-polarisation of each service corresponds to 100% of that service, and thus all the other scores are computed as a simple proportion, which is:

$$\frac{\text{score of single/dual polarisation}}{\text{score of quad polarisation}} = \frac{\text{percentage}}{100}$$

The percentage is rounded to the closest integer. For example, for the previous example of Built-up land, the score obtained for the quad-polarisation is 2.33. Therefore, the HH-polarisation, which obtained a score of 0.89, results in a percentage equal to 38%.

Finally, the *set-up* for the index computation is complete. The first input of the code is the wavelength of the sensor: if the service is related to the input spectral band an initial score of 100 is given to the sensor and it goes on to the next passage. If the spectral band is not commonly used for a certain service, the index is null.

This is done because, independently of the polarisation, that sensor would not be useful in the field of the considered service. In case the service is associated with the input spectral band, the second input is the polarisation. The index is computed as the average between 100 (coming from the input wavelength) and the entry of Table 11 corresponding to the input polarisation, named $pct_{polarisation}$. Hence the index is computed as:

$$I_{spectr} = \frac{100 + pct_{polarisation}}{2} \tag{32}$$

In case the sensor is capable of more than one polarisation or combination of single-polarisations, under the same conditions the highest index is taken as the final result.

2.4 Earth coverage index

The last index developed in the dissertation is the so-called Earth coverage index. It aims at quantifying the service visibility. The first step has been to associate all the services to their location on the Earth. To create a layer for each service, one or more parameters have been allocated to the nine EO services according to experience and datasets availability. As an example, the population density dataset is presented. This dataset provides an estimate of population density for the year 2020, based on counts consistent with national censuses and population registers with respect to relative spatial distribution. Each entry represents the inhabitants per square kilometre. To make it easier to represent the data, all values greater than 1000 (meaning that pixel corresponds to a geographic area with a population density greater than 1000 inhabitants per square kilometre) are set equal to 1000. This value was selected according to the SocioEconomic Data and Application Center (SEDAC) representation of the population density of the 2020 dataset, where all areas with a density>1000 persons/km^2 are represented with the darkest colour. The geographic data is shown using the command map show in Fig. 12.

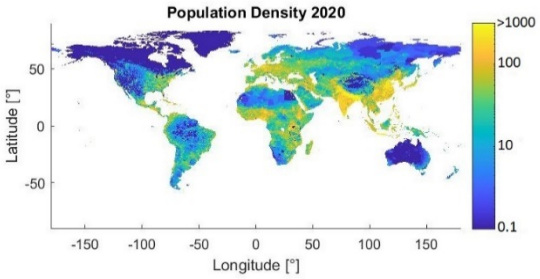

Fig. 12. Population density of the World, 2020

At this point, all the layers required to classify the services have been created and they are all 4320x8640 matrices containing the desired information. In this section, the allocation of the layers to each service is carried out.

For instance, the population density layer has been selected for the characterisation of the *Built-up land* service. Each entry ranges from 0 to 1000 inhabitants per square kilometre. Then, the values are normalised from 0 to 1 dividing by the maximum entry of the matrix. In the end, the final built-up land matrix contains all normalised values of population density.

Parameters have been selected for each Service, leading to the creation of nine matrices. A resume of the layers forming the final matrices for each EO service can be appreciated in Table.

SARs can provide high-resolution images regardless of weather conditions. It is essential to enhance this ability in the process of developing the Earth coverage index because about 67% of our planet's surface is typically covered with clouds. Decades of satellite observations and photographs show that clouds dominate the views, especially over the oceans, where usually less than 10% of the sky is clear of clouds at a given time. This percentage increases to 30% if lands are considered.

Basing on data collected by the Moderate Resolution Imaging Spectroradiometer (MODIS) on Aqua satellite (NASA), a cloud fraction map has been created as the average of the monthly data of 2020. The result is a 720x1440 matrix covering all latitudes and longitudes including the cloud coverage in each pixel with values ranging from 0 to 1. This has been included in the development of the index.

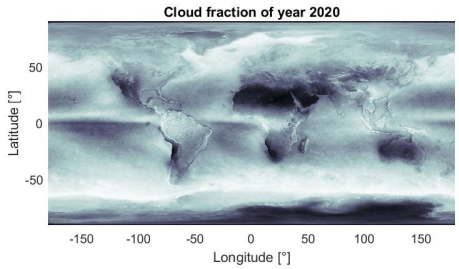

Fig. 13. Average cloud coverage, 2020

2.4.1 Index development

The first step for the Earth coverage index evaluation consists in the analysis of the ground track, discretised in points, considering the second zonal harmonic perturbation, introducing the corresponding acceleration in the derivation of the state.

For each integration step *i* of the ground track, the angular coefficients of the along and cross-ground track directions are computed. Then, the angle, α_i, between the cross-ground track direction and the equator is computed.

$$m_{along,i} = \frac{lat(i) - lat(i-1)}{lon(i) - lon(i-1)} \tag{33}$$

$$m_{cross,i} = -\frac{1}{m_{along}} \tag{34}$$

$$\alpha_i = \tan^{-1}\left(m_{cross}\right) \tag{35}$$

where $m_{along,i}$ and $m_{cross,i}$ are respectively the along-track and cross-track angular coefficients, *lat* and *lon* stand for the latitude and longitude coordinates coming from the ground track computation.

For passive sensors, four vertices of a rectangle can then be identified, whose sides are aligned with the along and cross ground track directions. This is done at each integration step according to the sensor swath width S^{deg}_{width}, expressed in Earth central angles, as:

$$lon_{right,i} = lon(i) + \frac{S^{\deg}_{width}\cos\left(\frac{\pi}{2} + \tan^{-1}\left(m_{along,i}\right)\right)}{2} \tag{36}$$

$$lat_{right,i} = lat(i) + \frac{S^{\deg}_{width}\cos\left(\frac{\pi}{2} + \tan^{-1}\left(m_{along,i}\right)\right)}{2} \tag{37}$$

$$lon_{left,i} = lon(i) - \frac{S^{\deg}_{width}\cos\left(\frac{\pi}{2} + \tan^{-1}\left(m_{along,i}\right)\right)}{2} \tag{38}$$

$$lat_{left,i} = lat(i) - \frac{S^{\deg}_{width}\cos\left(\frac{\pi}{2} + \tan^{-1}\left(m_{along,i}\right)\right)}{2} \tag{39}$$

where the sub-indices *left* and *right* stand for the points to the left and right of the ground track. The same four equations with *i*-1 instead of *i* are computed to obtain the other two points coordinates. The rectangle, identified by the four vertices, represents the ground observed region, hence, all the rectangles taken together form the strip of surface observed by the sensor during the repeat cycle. The rectangle is necessary for simulating the ground observed region by the whole swath width at each integration step.

For SAR sensors, because of their off-nadir observing capabilities, the following equations are used to identify the coordinates of the four points of the rectangle:

$$lon_{I,i} = lon(i) + d^{\deg}_{I}\cos\left(\frac{\pi}{2} + \tan^{-1}\left(m_{along,i}\right)\right) \tag{40}$$

$$lon_{I,i} = lon(i) + d^{\deg}_{I}\cos\left(\frac{\pi}{2} + \tan^{-1}\left(m_{along,i}\right)\right) \tag{41}$$

$$lon_{E,i} = lon(i) + d^{\deg}_{E}\cos\left(\frac{\pi}{2} + \tan^{-1}\left(m_{along,i}\right)\right) \tag{42}$$

$$lat_{E,i} = lat(i) + d^{\deg}_{E}\sin\left(\frac{\pi}{2} + \tan^{-1}\left(m_{along,i}\right)\right) \tag{43}$$

where d_i^{deg} and d_E^{deg} are the ground distances introduced in Eq. (19) expressed in Earth central angles and the sub-indices I and E stand for internal and external.

Graphical examples of the rectangles simulating the observed ground regions for both passive and SAR sensors are shown in Figs. and. Plus symbols represent the derived ground track points at each integration step and the circles correspond to the four vertices of the rectangle. The SAR modelled observed ground region reflects its side-looking geometry.

At this point, a method to associate these rectangles to the services layers is needed. A simple rotation matrix is used to rotate each of the four points of the angle α_i. The rotation is performed for computational efficiency reasons. Indeed, the reference frame is now aligned with the rectangle sides, thus enabling to easily fill the rectangle with a certain number of points depending on the integration step and sensor swath width. The number of filling points is such that the distance between them is approximately equal to the minimum distance between the pixels of the services layers. In this way, it is then possible to uniquely associate, at each integration step, the filling points of the rectangles to their related pixel position in a 432x864 matrix, once got back to the original reference frame. The dimension of 432x864

comes from a resizing of the original matrix by a factor of 10 for computational efficiency reasons.

Hence, the 432x864 matrix containing only the pixels detected by the satellite is obtained. Then, building from this matrix a corresponding 4320x8640 one, to be coherent with the service layers dimensions, the matrices of the pixels observed for each service layer is carried out.

As stated before, the Earth coverage index is based on the service visibility in a repeat cycle with respect to the total service visibility, and is computed as the number of service pixels observed, $n_{obs,Serv}$, with respect to the total number of pixels of such service, $n_{tot,Serv}$, as shown in (44):

$$I_{vis} = \frac{n_{obs,Serv}}{n_{tot,Serv}} 100 \tag{44}$$

The cloud coverage index I_{Cloud}, needed for the final Earth coverage index for passive sensors is modelled as:

$$I_{Cloud} = \frac{\sum_{n=1}^{n_{Cloud}} Pix_{Cloud,i} \Big/ Pix_{Cloud}^{\max}}{n_{Cloud}} 100 \tag{45}$$

where $Pix_{Cloud,i}$ stands for the cloud coverage value at step i, Pix^{max}_{Cloud} represents the maximum value of cloud coverage and n_{Cloud} is the number of cloud coverage pixels observed.

The Earth coverage index I_{Cov} for passive sensors is finally computed as:

$$I_{Cov} = I_{vis} I_{cloud} \tag{46}$$

while for active sensors $I_{Cov} = I_{vis}$.

3. Results

Sustainable development is the development that meets the needs of the present without compromising the ability of future generations to meet their own needs [48]. Earth Observation presents many advantages, which make it a critical source of data, allowing the monitoring of the progress towards the SDGs. In particular, EO gains some advantages over the traditional alternatives [48]:

- Coverage: the possibility of monitoring vast and remote countries.
- Objectivity: the measurements from satellites have a controlled range of error.
- Repeatability: the nature of satellite observations is periodic, allowing an important comparison of the measurements over time.
- Continuity: the continuous flow of EO data allows to build experience.
- Thematic detail: as the core of this dissertation states, the fields of application of EO sensors missions are numerous.
- Analysis-ready data: the data is organised according to defined standards, granting the possibility of immediate further analysis.
- Speed: the data is often available days or even hours after the acquirement, representing a huge advantage especially for the Hazards monitoring service.
- Affordability: the data is becoming more and more freely available due to the increase in commercial satellites.

The topic is currently one of the hot topics included in the future programmes of both space agencies and companies. To cite a few, the Group on Earth Observations (GEO) plays an instrumental role in the matter with its initiative EO4SDG, launched in 2016 in a close partnership with the UN agencies [9]. Inter-agency coordination needs to thank the efforts of the Committee on Earth Observation Satellites (CEOS), working with governments, academia, scientists, and the private sector to develop partnerships for the io-economic data which are relevant to the SDGs [49]. Concerning the latter, Enviro Atlas also provided a set of indicators that establish a way to help environmental indicators, contributing to targets of numerous goals, mostly SDG 6 for Clean Water, SDG 11 for Sustainable Cities and Communities and SDG 15 for Life on Land. EO-based data can indeed help fill the gaps existing in the current SDG indicators: multi-resolution spatial indicators, environmental indicators and indicators integrating societal or economic data, thus merging the three spheres of sustainable development. The spatial and temporal resolutions remain an issue for socio-economic data. EO data are now produced near-real-time, however, socio-economic data continue to be collected on multi-year or even decadal time frames, thus making the integration of data hard despite the quality of satellite data [49]. The United Nations Office for Outer Space Affairs (UNOOSA) holds a section of its website for the role of space in the achievement of the SDGs. For each goal, the place of space technologies is reported in bullet points resuming the main support of satellites [11]. Basing on the possibilities listed by UNOOSA for each goal and keeping in mind the works carried out by GEO, CEOS and ESA, a table that better suits the goal of the current dissertation has been developed [9] [7] [11]. Because of the need to assign a final result basing on the EO services, Table 14 describes the role that each service can have to support each Activity. The Activities correspond to the read justed possibilities listed by UNOOSA which are connected to Earth Observation (the other applications are left out of the analysis). For each Activity, the role of each service to its support has been identified through a score from 0 to 5. Hereafter the legend of these scores is reported:

- 0 corresponds to the service cannot support at all the Activity.

- 1 corresponds to the service is marginal for the achievement of the Activity.
- 2 corresponds to the service can poorly support the Activity.
- 3 corresponds to the service can moderately support the Activity.
- 4 corresponds to the service can strongly support the Activity.
- 5 corresponds to the service is fundamental for the Activity achievement.

The last row of each SDG contains the total score of each service with the weighted sum of the scores of such service for each activity. This means that each score is multiplied by the weight of the corresponding Activity and then summed to the other ones multiplied in turn by their weight. As an example, for SDG number 1, the total score of Built-upland is 2.3, which is the result of (1·0.3 + 0·0.3 + 5·0.4). As can be easily noticed, the sum of the weights of each Goal is 1, for reasons of objectivity. In such a way, the authors contribution is limited to the definition of the scores from 0 to 5 assigned to the services and to the division of weights assigned to the Activities.

Finally, in the first cell of the SDGs final row, the SDGs total score is reported as the sum of the services total scores. In the case of SDG number 1, the total is 7.5, which is given by the sum of (2.3 + 0.9 + 1.2 + 0.3 + 1.3 + 0 + 0 + 0 + 1.5). This number shall be utilised for the computation of the final index. It is important to highlight that the numbers in the table have been selected by the authors of the dissertation based on literature and experience. Further work is needed to consolidate the validity of such quantities, possibly employing surveys and or stakeholders advice for the update of the table.

3.1 SDG indices development

As stated in the previous section, Table 14 reports the link between the EO services and the SDGs. This is fundamental for the achievement of the final indices that are the core of the dissertation: these allow quantifying the social contribution of a given mission using the SDGs. The outputs of the modelling are the four modelled indices, which are the spatial resolution index, the temporal resolution index, the spectral efficiency index and finally the Earth coverage index. Hereafter the connection among these indices and the SDGs is reported.

Two indices are developed for each SDG, resulting in a total of 34 indices. The first series of indices represents the contribution that each mission can give to the SDGs with respect to the given service maximum capability. These indices are named $I_{SDG1,rel}$, $I_{SDG2,rel}$ etc., where the number in the subscript stands for the SDG taken into account. The second set, on the other hand, is lowered because it considers the maximum value among all the services capabilities for the Goals, leading to indices proportional to the doughnut chart in Fig. 14. These are denoted with $I_{SDG1,abs}$, $I_{SDG2,}$abs, etc.

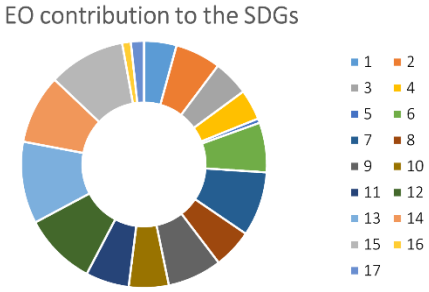

Fig. 14. EO contribution to the SDGs

It is clear that for some Goals the role of EO is marginal, while for others it is essential.. The first step, in both cases, is to obtain a final score for each service which is modelled as the average of the four indicators. Each of these numbers is then multiplied by its corresponding number in Table 14 for each Goal (i.e. for SDG number 1, the Built-up land index is multiplied by 2.3, the Agriculture index is multiplied by 0.9 and so on) and these products are summed. At this point, the denominator to obtain the two series of indices is different. In the first set, the denominator is the total of the considered Goal, as reported in Table 14. In the second set, the denominator is always the total of Goal 13 (that is equal to 18.8), considering the maximum EO contribution. Hence, the formulas are:

$$I_{SDGX,rel} = \frac{I_{blt}N_{blt,X} + I_{agr}N_{agr,X} + \ldots + I_{haz}N_{haz,X}}{Total\ of\ Goal\ X} \quad (47)$$

$$I_{SDGX,abs} = \frac{I_{blt}N_{blt,X} + I_{agr}N_{agr,X} + \ldots + I_{haz}N_{haz,X}}{Total\ of\ maximum\ Goal} \quad (48)$$

Whilst the indices of the first set can have any value between 0 and 100, the second set of indices are intrinsically unable to reach the maximum value of 100, except for the one corresponding to the SDG with the maximum sum of the services scores, which is SDG 13, with a total of 18.8. The other indices can reach a maximum value which is proportional to their sum of the services scores because this represents the contribution that EO can give to such Goal.

3.2 Application to Copernicus

In the following section, the European Earth Observation program Copernicus is evaluated according to the developed indices and the SDGs. The complete derivation of the social outcomes is reported only for the Sentinel-1. Then, the cumulative result of the program is presented.

Sentinel-1 represents the European Radar Observatory, was designed and developed by ESA and funded by the European Commission (EC). It consists of

a constellation of two satellites, Sentinel-1A and Sentinel-1B, sharing the same orbital plane with a 180° orbital phasing difference. The satellites carry a C-band SAR sensor that provides data continuity to ERS and Envisat SAR missions. The Sentinel-1 mission is specifically designed to systematically acquire and routinely provide data and information products to Copernicus Marine, Land Monitoring and Emergency Management services as well as to national user services. These services focus on operational applications such as the observation of the marine environment, the surveillance of maritime transport zones, as well as the monitoring of land surfaces and mapping in support of crises such as natural disasters and humanitarian aids [13]. The two satellites were launched in 2014 and 2016, while in the next years the launches of Sentinels 1C and 1D are scheduled to join the Sentinel-1 constellation [50]. All the orbital and sensors parameters needed for the indices evaluation are reported in Table 12 [13].

Table 12. Orbital and sensor parameters for Sentinel-1

Variable	Sentinel-1
Revolutions in a repeat cycle	175
Days for a repeat cycle	12
Altitude	693
Sensors swath width	375 km
Antenna azimuthal length	12.3 m
Look angle	46 deg
Bandwidth	50 MHz
Operative band	C
Polarisation	HH,VV,HV,VH
Inclination	98.18 deg
Start longitude at the equator	192 deg

Sentinel-1 C-band SAR sensors can operate in four different operating modes. The one considered for this analysis is the Stripmap mode, however, it is worth mentioning that no significant differences are present in the final indices evaluation for the different operating modes. The four indices for each service are presented in Fig. 15 and Table 13 the averaged service indices can be appreciated. In the diagram shown in Fig. 16 and Fig. 17 the final contribution of Sentinel-1 in monitoring and achieving the SDGs is figured out through the $I_{SDG,rel}$ and the $I_{SDG,abs}$ indices.

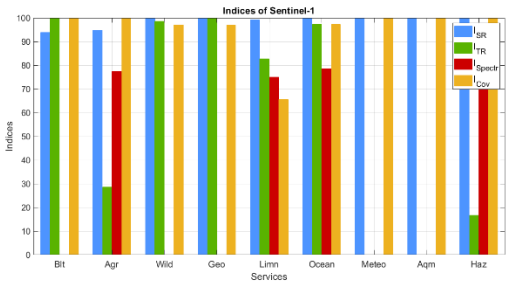

Fig. 15. Spatial and temporal resolution, spectral efficiency and Earth coverage indices for Sentinel-1

Table 13. Service indices of Sentinel-1

Service	$I_{Service}$
Built-up land	0
Agriculture	75.22
Wild nature	0
Geology	0
Limnology	80.64
Oceanography	93.22
Meteorology	0
Air Quality Monitoring	0
Hazards monitoring	72.92

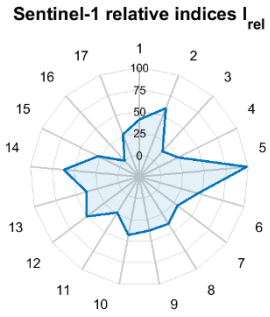

Fig. 16. Sentinel-1 contribution in terms of I_{rel}

As it can be appreciated, Sentinel-1 gains very high service indices, but limited only to four services, according to the SAR sensor operative band. In terms of SDGs contribution, the Goals 2, 12, 13, and 14 result to be particularly assisted by the mission considered.

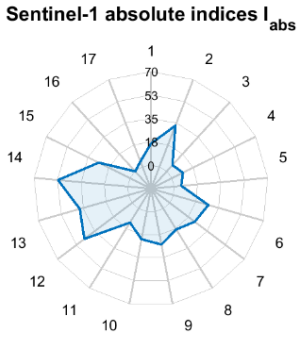

Fig. 17. Sentinel-1 contribution in terms of I_{abs}

3.3 Earth coverage index

Carrying out the analysis for the whole Copernicus mission, some results are here presented. The indices obtained for the Services are reported in Fig. 18.

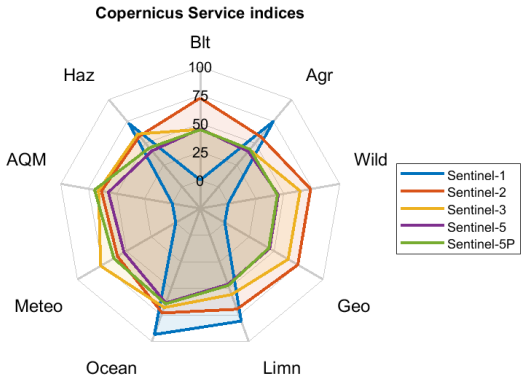

Fig. 18. Copernicus service indices

The aspect that can be immediately noticed is the difference between passive and active sensors. While passive sensors result in worse but broader applications, the active instrument (C-SAR on Sentinel-1 satellite) has more specific applications with relative much higher indices. According to Table 14, Earth Observation can contribute more to Goal 13 (Climate Action), followed by Goal 15 (Life on Land) and Goal 12 (Responsible Consumption and Production). The contribution of the Copernicus program to these goals is reported in Fig. 19, Fig. 20 and Fig. 21. This result can be computed for every other Goal, however, these are deemed more relevant. From the Copernicus analysis, it turns out that, even if good results are gained, they can and must be improved in the future.

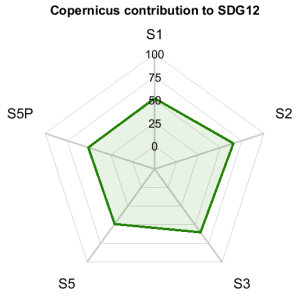

Fig. 19. Copernicus contribution to Goal 12

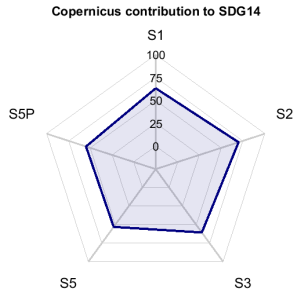

Fig. 20. Copernicus contribution to Goal 14

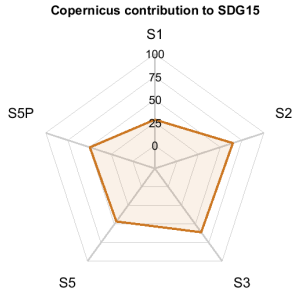

Fig. 21 Copernicus contribution to Goal 15

4. Conclusions

In this paper, the complete derivation of a tool for the evaluation of the social value assessment of EO missions is described. Starting from technical parameters of both the satellite and the payloads, a rigorous evaluation of the mission contribution to several services has been performed. After that, linking the services to the SDGs, the social rating is made possible. According to the achieved results, several considerations can be made concerning passive and SAR sensors. Passive instruments are characterised by a high versatility in terms of services supply, while SARs provide only certain services according to their operative band. However, the latter can obtain higher services scores than passive sensors, especially if operating in full-polarimetric modes. Though, the advent of hyper-spectral sensors is filling the gap of passive instruments, providing break through imaging capabilities in terms of spectral efficiency. According to the study, from a social

contribution point of view, it turns out that passive instruments are the ones that support the SDGs more effectively, thanks to their versatility. However, the next future of EO satellite sensors is going to be still characterised by a combination of these two kinds of imaging technologies, and the reason can be found in the complementarity of the attainable data. Criticalities of the work are in general related to the intrinsic difficulty in quantifying something not directly measurable like social benefits. The boundaries lability of service requirements, on which the four technical indices are based, represents a slight problem since they play a crucial role in the definition of the final score. Taking the arithmetic average of the four indices, rather than a weighted one, may results in a loss of information, depending on the service and the SDG Activity considered. To carry out a more accurate analysis, certain services could be split into sub-services (e.g. Built-up land in Houses, Transport, Infrastructures or Limnology in Glaciers, Rivers and Lakes, In-land Seas), to facilitate the contribution allocations to each Goal Activity. Another source of uncertainty is represented by Table 2.1. As already stated, further work is needed to consolidate the validity of the assigned quantities, also employing surveys and/or stakeholders advice. Finally, the flexibility of the sensors during the imaging process, such as the different operating modes, results in challenging proper modelling. As stated in the dissertation, the analysis is only applied to circular repeating Sun-synchronous orbits missions in LEO, belonging to the EO class, taking into account the second zonal harmonic as the only perturbation. From a payload point of view, passive and SAR sensors only are analysed. Future developments of this study, besides including other types of perturbation such as the atmospheric drag, shall then consider extending both the evaluable sensors types and mission orbits. Lidars, radar altimeters and microwave radiometers shall be included in the analysis to achieve an optimal modelling capacity for what concerns sensors, while geostationary as well as elliptical orbits could be added in the study to gain a complete modelling coverage from an orbit class point of view. Finally, the work shall be extended to navigation and telecommunication applications, to achieve a global evaluation of all the space applications for Earth. The analysis shall be extended to other space missions classes, such as Science and Exploration or Safety and Security. However, the identification of proper services and their contributions allocation to the SDGs would encounter significant obstacles. To achieve a comprehensive evaluation, other space missions features shall be taken into account, such as their footprint in terms of orbit crowding and space debris, orbit maintenance requirements, readiness from the acquisition and open-source availability of data, international cooperation fostering. In parallel, efforts should be made in understanding and properly integrating to the already identified services the limitless potential of space-based data that downstream gateways highlight day by day.

Acknowledgements

The research leading to these results has received funding from the European Research Council (ERC) under the European Unions Horizon 2020 research and innovation program as part of project COMPASS (Grant agreement No. 679086).

Appendix A (Contribute that each service can give to the activities related to the SDGs)

Table 14. Contribute that each service can give to the activities related to the SGDs

Goal	Activity	Blt	Agr	Wild	Geo	Limn	Ocean	Meteo	AQM	Haz	Weight (0-1)
1	Natural disaster	1	0	0	0	0	0	0	0	5	0.3
	Natural resources	0	3	4	1	3	0	0	0	0	0.3
	Mapping populated areas	5	0	0	0	1	0	0	0	0	0.4
Total		2.3	0.9	1.2	0.3	1.3	0	0	0	1.5	
2	Crop productivity	0	5	0	0	3	0	3	1	0	0.5
	Livestock management	0	5	2	0	2	0	0	0	0	0.5
Total		0	5	1	0	2.5	0	1.5	0.5	0	
3	Prevention of diseases	2	0	2	0	0	0	0	2	0	0.3
	Reduction air pollution	5	0	0	0	0	0	0	5	0	0.4
	Emergency response service	3	0	0	0	0	0	0	0	5	0.5
Total		3.5	0	0.6	0	0	0	0	2.6	1.5	

4	Educational infrastructures	5	0	0	0	0	0	0	0	0	0.5
	Data object production	1	1	1	1	1	1	1	1	1	0.5
Total		3	0.5	0.5	0.5	0.5	0.5	0.5	0.5	0.5	
5	Assistance violence victims	0	0	0	0	0	1	0	0	0	1
Total		0	0	0	0	0	0	0	0	0	
6	Water quality	4	0	0	0	5	0	0	0	0	0.4
	Meteo forecast	0	0	0	0	0	0	5	0	0	0.2
	Water resources	0	5	5	0	5	0	0	2	0	0.4
Total		1.6	2	2	0	4	0	1	0.8	0	
7	Infrastructures	5	0	0	0	0	0	0	0	0	0.3
	Renewable energy resource	4	0	2	3	5	2	3	0	0	0.7
Total		4.3	0	1.4	2.1	3.5	1.4	2.1	0	0	
8	Global GDP growth	1	1	1	1	1	1	1	1	1	1
Total		1	1	1	1	1	1	1	1	1	
9	Infrastructures	5	0	0	0	2	0	1	0	2	0.5
	Innovative technologies	4	4	1	2	1	2	1	0	0	0.5
Total		4.5	2	0.5	1	1.5	1	1	0	1	
10	Connectivity and info access	3	0	0	0	0	0	0	0	0	0.4
	Opportunities development	2	4	3	0	2	1	0	2	2	0.4
	Migration	2	0	1	0	1	3	0	0	1	0.2
Total		2.4	1.6	1.4	0	1	1	0	0.8	1	
11	Urban planning	5	2	0	0	0	0	0	2	1	0.3
	Smart cities	5	0	1	0	2	0	0	2	0	0.4
	Infrastructures	5	0	1	0	2	0	0	0	1	0.2
	Air quality	0	0	0	0	0	0	2	5	5	0.1
Total		4.5	0.6	0.6	0	1.2	0	0.2	1.9	1	
12	Natural resources	0	0	5	4	4	4	0	0	3	0.4
	Smart agriculture	0	5	0	0	2	0	3	1	0	0.3
	Waste management	4	0	0	3	5	5	0	1	0	0.3
Total		1.2	1.5	2	2.5	3.7	3.1	0.9	0.6	1.2	
13	Climate change	3	1	5	2	4	5	5	3	0	0.6
	Disaster check	0	0	0	0	0	0	0	0	5	0.4
Total		1.8	0.6	3	1.2	2.4	3	3	1.8	2	
14	Marine ecosystem	3	0	0	0	5	5	0	1	1	0.3
	Fishing	2	0	0	0	5	5	2	0	0	0.3
Total		3.1	0	0	0	5	5	1.8	0.3	0.7	
15	Forests check	1	3	5	5	4	0	3	2	4	0.4
	Biodiversity safeguard	0	3	5	0	0	0	3	2	0	0.5
	Poaching	2	0	0	1	0	0	0	0	1	0.1
Total		0.6	2.7	4.5	2.1	1.6	0	2.7	1.8	1.7	
16	Conflict check	2	0	0	0	0	0	0	0	0	1
Total		2	0	0	0	0	0	0	0	0	

17	International activities	4	3	0	0	0	0	0	0	0	1
Total		2	1	0	0	0	0	0	0	0	

References

In the text

Indicate references by number(s) in square brackets in line with the text. The actual authors can be referred to, but the reference number(s) must always be given.

Example: "..... as demonstrated [3,6]. Barnaby and Jones [8] obtained a different result ...."

List of references

Number the references (numbers in square brackets) in the list in the order in which they appear in the text.

Examples:

Reference to a journal publication:

[1] J. van der Geer, J.A.J. Hanraads, R.A. Lupton, The art of writing a scientific article, J. Sci. Commun. 163 (2010) 51–59.

Reference to a conference/congress paper:

Y.-W. Chang, J.-S. Chern, Ups and Downs of Space Tourism Development in 60 Years from Moon Register to SpaceShipTwo Crash, IAC-15-E4.2.8, 66th International Astronautical Congress, Jerusalem, Israel, 2015, 12 – 16 October.

Reference to a book:

[2] W. Strunk Jr., E.B. White, The Elements of Style, fourth ed., Longman, New York, 2000.

Reference to a chapter in an edited book:

[3] G.R. Mettam, L.B. Adams, How to prepare an electronic version of your article, in: B.S. Jones, R.Z. Smith (Eds.), Introduction to the Electronic Age, E-Publishing Inc., New York, 2009, pp. 281–304.

Reference to a website:

[4] E. Mack, Could Virgin Galactic's Spaceport America be put up for sale? 23 February 2015, http://www.gizmag.com/spaceport-america-hits-nags/36200/, (accessed 30.04.16).